NASA/CR-97- 205827

FINAL
IN-93-CR
10IT.

Final Report for

Grant No. NCC8-82

An Analysis of Gamma-ray Burst Time Profiles from the Burst And Transient Source Experiment

John Patrick Lestrade

Mississippi State University

Principal Investigator

November, 1996

Final Report for

Grant No. NCC8-82

An Analysis of Gamma-ray Burst Time Profiles from the Burst And Transient Source Experiment

by

John Patrick Lestrade
Professor of Physics and Astronomy
Mississippi State University
Mississippi State, Mississippi, 39762

I. Introduction.

This proposal requested funding to measure the durations of gamma-ray bursts (GRB) in the 4B catalog as well as to study the structure of GRB time profiles returned by the Burst And Transient Source Experiment (BATSE) on board the Compton Gamma-Ray Observatory. The duration (T90) was to be measured using the same techniques and algorithms developed by the principal investigator for the 3B data. The profile structure studies fall into the two categories of variability and fractal analyses.

IIA. Duration Measurements

As part of this contract, we agreed to measure the burst durations for the 4B catalog. The measurement of gamma-ray burst durations is significant for several reasons but especially so since duration is the only GRB characteristic which clearly shows that these objects fall into 2 distinct groups. Burst hardness also could be argued to be a parameter of equal importance, but a histogram of hardness alone does not show any grouping or clustering. However, we recently showed (Dezalay, Lestrade, et al, 1996: attached herein) that the hardness-duration diagram contains more information than previously believed. It was common knowledge that shorter bursts were harder, on average, than longer bursts. This anti-correlation has been well-documented. We found, however, that there is a secondary relationship hidden in the longer bursts. That is, we present clear evidence for a positive correlation in bursts whose durations (T90) are longer than 2 secs. This new finding has been confirmed by the work of Horack et al (1996). These new results make an accurate and dependable determination of T90 all the more important.

IIB. Results of Duration Measurements

There were a total of 429 bursts used in this study. These included trigger numbers between 3177 and 5483 (inclusive). As was true in previous burst catalogs, data gaps (caused by the failure of the onboard tape recorders as well as other normal interruption of burst data accumulation) restricted the availability of some of the BATSE data types. Table I lists all 429 bursts with the data types that were used to determine their durations. Appropriate comments will be made in the comments file, where the gaps restricted the T90 measure. The data type codes are l=discla, p=preburst, s=discsc, t=tte, and b=disclb. Disclb was used only to fill in gaps when discla data were unavailable. This was necessary for 65 GRB's.

Two sample pages of output from our duration measuring program are included in this report as Figures 1-2.

Of the 429, approximately 65 were short enough to require TTE data for accurate T90 determination but their TTE datasets were missing packets.

Figure 3 presents the duration histogram for these 429 GRB's. As expected, the T90 bimodality is still present.

III. Fractal Algorithms

Our current work in this interesting new area of mathematical physics concerns the application of several proven algorithms to GRB time profiles. In this effort I have the help of Yan Yuan, a PhD graduate student at MSU (See attached résumé). As part of his dissertation, Yan is looking for evidence of scale invariance embedded in the burst time profiles. The problem with studies of these kind is that noise and short data sets (both characteristics of GRB time profiles) obfuscate the results. However, that doesn't mean that we should give up. There are many different fractal algorithms – with different areas of applicability. We are searching for the correct algorithm to unlock the secrets of GRB. This search is especially important since standard methods of analysis have failed at almost every turn when applied to these cosmic events.

5. Bibliography.

Dezalay, J-P, J. P. Lestrade, et al, The Hardness-Duration Diagram of Gamma-Ray Bursts, Astrop. J., **471**, L27-30.

Horack, J., et al (1996) Astrop. J, (submitted).

Table I: Data Types used for each Burst Profile.

Trig#	DLA	Preb	DSC	TTE	DLB	Trig#	DLA	Preb	DSC	TTE	DLB
3177	l	p	s	-	-	3764	l	p	s	-	-
3178	l	p	s	-	-	3765	l	p	s	-	-
3193	l	p	s	-	-	3766	l	p	s	-	-
3200	-	p	-	-	b	3767	-	p	s	-	b
3212	l	p	s	-	-	3768	l	p	s	-	-
3215	l	p	s	-	-	3770	l	p	s	t	-
3217	l	p	s	-	-	3771	l	p	s	-	-
3218	l	p	s	t	-	3772	l	p	s	-	-
3220	l	p	s	-	-	3773	l	p	s	-	-
3227	l	p	s	-	-	3774	l	p	s	t	-
3229	l	p	s	-	-	3775	-	p	-	-	b
3237	l	p	s	-	-	3776	l	p	s	-	-
3238	l	p	s	-	-	3779	l	p	s	-	-
3240	-	p	s	t	b	3781	l	p	s	-	-
3241	l	p	s	-	-	3782	l	p	s	t	-
3242	l	p	s	-	-	3788	l	p	s	-	-
3243	-	p	s	t	b	3789	l	p	s	-	-
3245	l	p	s	-	-	3790	-	p	s	t	b
3246	l	p	s	-	-	3791	l	p	s	t	-
3247	l	p	s	-	-	3792	l	p	s	-	-
3248	l	p	s	-	-	3796	-	p	-	-	b
3249	-	p	s	t	b	3797	-	p	-	t	b
3250	l	p	s	-	-	3799	l	p	s	t	-
3251	l	p	s	-	-	3800	l	p	s	-	-
3253	l	p	s	-	-	3801	l	p	s	-	-
3255	l	p	s	-	-	3803	l	p	s	t	-
3256	l	p	s	-	-	3804	-	p	s	t	b
3257	l	p	s	-	-	3805	l	p	s	-	-
3259	l	p	s	-	-	3806	l	-	-	-	-
3266	l	p	s	t	-	3807	l	p	s	-	-
3267	l	p	s	-	-	3810	l	p	s	t	-
3269	l	p	s	-	-	3811	l	p	s	-	-
3273	l	p	s	-	-	3812	l	p	s	-	-
3276	l	p	s	-	-	3814	l	p	s	-	-
3278	l	p	s	-	-	3815	l	p	s	-	-

Table I (cont.): Data Types used for each Burst Profile.

Trig#	DLA	Preb	DSC	TTE	DLB	Trig#	DLA	Preb	DSC	TTE	DLB
3279	l	p	s	-	-	3819	l	p	s	-	-
3280	l	p	s	-	-	3840	l	p	s	t	-
3282	l	p	s	t	-	3843	l	p	s	-	-
3283	l	p	s	-	-	3846	-	p	s	t	b
3284	l	p	s	-	-	3848	-	p	s	t	b
3286	l	p	s	-	-	3853	l	p	s	-	-
3287	l	p	s	-	-	3857	-	p	-	-	b
3289	-	p	s	-	b	3860	l	p	s	-	-
3290	l	p	s	-	-	3864	l	p	s	-	-
3291	-	p	-	t	b	3866	l	p	s	-	-
3292	l	p	s	-	-	3867	l	p	s	t	-
3293	l	p	s	-	-	3868	l	p	s	-	-
3294	l	p	s	t	-	3869	l	p	s	-	-
3295	-	p	s	t	b	3870	l	p	s	-	-
3296	-	p	s	t	b	3871	l	p	s	-	-
3297	l	p	s	t	-	3875	l	p	s	-	-
3298	-	p	-	t	b	3879	l	p	s	-	-
3299	-	p	s	t	b	3885	-	p	s	-	b
3301	l	p	s	-	-	3886	l	p	s	-	-
3303	l	p	s	-	-	3887	l	p	s	-	-
3305	-	p	s	t	b	3888	l	p	s	t	-
3306	l	p	s	-	-	3889	l	p	s	t	-
3307	l	p	s	-	-	3890	l	p	s	-	-
3308	l	p	s	-	-	3891	l	p	s	-	-
3311	-	p	-	t	b	3892	l	p	s	-	-
3319	l	p	s	-	-	3893	l	p	s	-	-
3320	l	p	s	-	-	3894	l	p	s	t	-
3321	l	p	s	-	-	3895	l	p	s	-	-
3322	l	p	s	-	-	3897	-	p	s	-	b
3323	l	p	s	t	-	3899	l	p	s	-	-
3324	l	p	s	-	-	3900	l	p	s	-	-
3325	-	p	s	-	b	3901	l	p	s	-	-
3328	-	p	s	-	b	3902	l	p	s	-	-
3330	l	p	s	-	-	3903	l	p	s	-	-
3335	l	p	s	t	-	3904	l	p	s	t	-

Table I (cont.): Data Types used for each Burst Profile.

Trig#	DLA	Preb	DSC	TTE	DLB	Trig#	DLA	Preb	DSC	TTE	DLB
3336	l	p	s	-	-	3905	l	p	s	-	-
3337	-	p	s	-	b	3906	l	p	s	-	-
3338	l	p	s	t	-	3908	l	p	s	-	-
3339	l	p	s	-	-	3909	l	p	s	-	-
3340	l	p	s	t	-	3910	l	p	s	t	-
3342	l	p	s	t	-	3911	l	p	s	-	-
3345	l	p	s	-	-	3912	l	p	s	-	-
3347	l	p	s	-	-	3913	l	p	s	-	-
3349	l	p	s	-	-	3914	l	p	s	-	-
3350	l	p	s	-	-	3915	l	p	s	t	-
3351	l	p	s	-	-	3916	l	p	s	-	-
3352	l	p	s	-	-	3917	l	p	s	-	-
3356	l	p	s	-	-	3918	l	p	s	-	-
3357	l	p	s	-	-	3919	l	p	s	t	-
3358	l	p	s	-	-	3921	l	p	s	t	-
3359	l	p	s	t	-	3924	l	p	s	-	-
3360	-	p	s	-	b	3926	l	p	s	-	-
3361	-	p	s	-	b	3927	-	p	-	-	b
3364	l	p	s	-	-	3929	l	p	s	-	-
3366	-	p	s	-	b	3930	l	p	s	-	-
3369	l	p	s	-	-	3931	l	p	s	-	-
3370	l	p	s	-	-	3932	-	p	-	-	b
3374	l	p	s	t	-	3935	l	p	s	-	-
3378	l	p	s	t	-	3936	l	p	s	t	-
3379	l	p	s	t	-	3937	l	p	s	-	-
3384	l	p	s	t	-	3938	l	p	s	-	-
3385	-	p	s	-	b	3939	l	p	s	t	-
3403	l	p	s	-	-	3940	l	p	s	-	-
3405	l	p	s	-	-	3941	l	p	s	-	-
3406	l	p	s	-	-	3954	l	p	s	-	-
3407	l	p	s	-	-	4039	l	p	s	-	-
3408	l	p	s	-	-	4048	l	p	s	-	-
3410	l	p	s	t	-	4095	l	p	s	-	-
3412	l	p	s	t	-	4146	l	p	s	-	-
3415	l	p	s	-	-	4157	l	p	s	-	-

Table I (cont.): Data Types used for each Burst Profile.

Trig#	DLA	Preb	DSC	TTE	DLB	Trig#	DLA	Preb	DSC	TTE	DLB
3416	l	p	s	-	-	4216	l	p	s	-	-
3431	l	p	s	t	-	4251	l	p	s	-	-
3436	l	p	s	-	-	4256	l	p	s	-	-
3437	l	p	s	t	-	4312	l	p	s	-	-
3439	l	p	s	-	-	4327	l	p	s	-	-
3440	-	p	s	-	b	4350	l	p	s	-	-
3441	l	p	s	t	-	4368	l	p	s	-	-
3442	-	p	-	-	b	4388	l	p	s	-	-
3443	-	p	-	-	b	4462	-	p	s	-	b
3448	l	p	s	-	-	4469	l	-	-	-	-
3449	-	p	s	t	b	4556	l	p	s	-	-
3450	-	p	-	t	b	4569	l	p	s	-	-
3453	l	p	s	-	-	4636	-	p	s	-	b
3458	l	p	s	-	-	4649	-	p	-	-	b
3464	l	p	s	-	-	4653	l	p	s	-	-
3465	l	p	s	-	-	4660	l	p	s	t	-
3466	l	p	s	-	-	4701	l	p	s	-	-
3467	l	p	s	-	-	4710	l	p	s	-	-
3471	l	p	s	-	-	4744	l	p	s	-	-
3472	l	p	s	-	-	4745	l	p	s	-	-
3473	l	-	s	-	-	4757	-	p	-	-	b
3476	l	p	s	-	-	4761	-	p	-	t	b
3477	l	p	s	t	-	4776	l	p	s	-	-
3480	l	p	s	t	-	4807	l	p	s	-	-
3481	l	p	s	-	-	4814	l	p	s	-	-
3485	l	p	s	-	-	4871	l	p	s	-	-
3486	l	p	s	-	-	4898	-	p	-	-	b
3487	l	p	s	t	-	4939	l	p	s	-	-
3488	l	p	s	-	-	4955	l	p	s	t	-
3489	l	p	s	-	-	4959	l	p	s	-	-
3491	l	p	s	-	-	5079	l	p	s	t	-
3492	l	p	s	-	-	5080	l	p	s	-	-
3493	l	p	s	-	-	5123	l	p	s	t	-
3494	l	p	s	-	-	5206	l	p	s	t	-
3499	-	p	s	-	b	5212	l	p	s	t	-
3502	l	p	s	t	-	5255	l	p	s	-	-

Table I (cont.): Data Types used for each Burst Profile.

Trig#	DLA	Preb	DSC	TTE	DLB	Trig#	DLA	Preb	DSC	TTE	DLB
3503	l	p	s	-	-	5277	l	p	s	t	-
3505	l	p	s	-	-	5299	l	p	s	-	-
3509	l	p	s	-	-	5304	l	p	s	-	-
3510	l	p	s	t	-	5305	l	p	s	-	-
3511	l	p	s	-	-	5316	l	p	s	t	-
3512	l	p	s	-	-	5337	l	-	-	-	-
3514	l	p	s	-	-	5339	l	p	s	-	-
3515	l	p	s	-	-	5377	-	p	-	-	b
3516	l	p	s	-	-	5379	l	p	s	-	-
3523	l	p	s	-	-	5387	l	p	s	-	-
3527	l	p	s	-	-	5389	l	p	s	-	-
3528	l	p	s	-	-	5392	-	p	-	-	b
3529	-	p	s	-	b	5407	l	p	s	-	-
3530	l	p	s	-	-	5409	l	p	s	-	-
3537	-	p	s	-	b	5410	l	p	s	-	-
3545	l	p	s	t	-	5411	l	p	s	-	-
3552	l	p	s	-	-	5412	l	p	s	-	-
3567	l	p	s	-	-	5413	l	p	s	-	-
3569	l	p	s	-	-	5415	l	p	s	-	-
3571	l	p	s	-	-	5416	l	p	s	-	-
3580	l	p	s	-	-	5417	l	p	s	-	-
3585	l	p	-	t	-	5418	-	p	s	-	b
3588	l	p	s	-	-	5419	l	p	s	-	-
3590	-	p	-	-	b	5420	l	p	s	-	-
3593	l	p	s	-	-	5421	l	p	s	-	-
3594	l	-	s	-	-	5423	l	p	s	-	-
3595	-	p	-	-	b	5425	l	p	s	-	-
3598	l	p	s	-	-	5427	l	p	s	-	-
3606	l	p	s	t	-	5428	l	p	s	-	-
3608	l	p	s	-	-	5429	l	p	s	-	-
3611	l	p	s	-	-	5432	-	p	-	-	b
3618	l	p	s	-	-	5433	l	p	s	-	-
3634	l	p	s	-	-	5434	l	p	s	-	-
3637	l	p	s	-	-	5436	l	p	s	-	-
3639	l	p	s	-	-	5439	l	p	s	-	-
3640	l	p	s	t	-	5443	-	p	s	-	b

Table I (cont.): Data Types used for each Burst Profile.

Trig#	DLA	Preb	DSC	TTE	DLB	Trig#	DLA	Preb	DSC	TTE	DLB
3642	l	p	s	-	-	5444	l	p	s	-	-
3643	l	p	s	t	-	5446	l	p	s	-	-
3644	l	p	s	t	-	5447	l	p	s	-	-
3647	l	p	s	-	-	5448	l	p	s	t	-
3648	l	p	s	-	-	5450	l	p	s	-	-
3649	l	p	s	-	-	5451	l	p	s	-	-
3651	-	p	-	-	b	5452	l	p	s	-	-
3652	l	p	s	-	-	5453	l	p	s	t	-
3654	l	p	s	-	-	5454	l	p	s	-	-
3655	l	p	s	-	-	5456	l	p	s	-	-
3657	-	p	-	-	b	5457	l	p	s	-	-
3658	l	p	s	-	-	5458	l	p	s	t	-
3662	l	p	s	-	-	5459	l	p	s	t	-
3663	l	p	s	-	-	5461	l	p	s	-	-
3664	l	p	s	-	-	5462	l	p	s	-	-
3665	l	p	s	t	-	5463	l	p	s	-	-
3668	l	p	s	t	-	5464	l	p	s	-	-
3671	l	p	s	-	-	5465	l	p	s	t	-
3709	l	p	s	t	-	5466	l	p	s	-	-
3711	l	p	s	-	-	5467	l	p	s	t	-
3717	l	p	s	-	-	5468	-	p	s	-	b
3720	l	p	s	-	-	5469	l	p	s	t	-
3722	l	p	s	-	-	5470	l	p	s	-	-
3728	l	p	s	t	-	5471	l	p	s	t	-
3733	l	p	s	-	-	5472	l	p	s	-	-
3734	-	p	s	-	b	5473	l	p	s	-	-
3735	l	p	s	t	-	5474	l	p	s	-	-
3736	l	p	s	t	-	5475	l	p	s	-	-
3737	l	p	s	t	-	5476	l	p	s	-	-
3740	l	p	s	-	-	5477	l	p	s	-	-
3742	l	p	s	-	-	5478	l	p	s	-	-
3745	l	p	s	-	-	5479	l	p	s	-	-
3750	-	p	s	t	b	5480	l	p	s	-	-
3751	l	p	s	t	-	5482	l	p	s	-	-
3758	-	p	s	-	b	5483	l	p	s	t	-
3762	-	p	s	t	b						

LPS_3177.

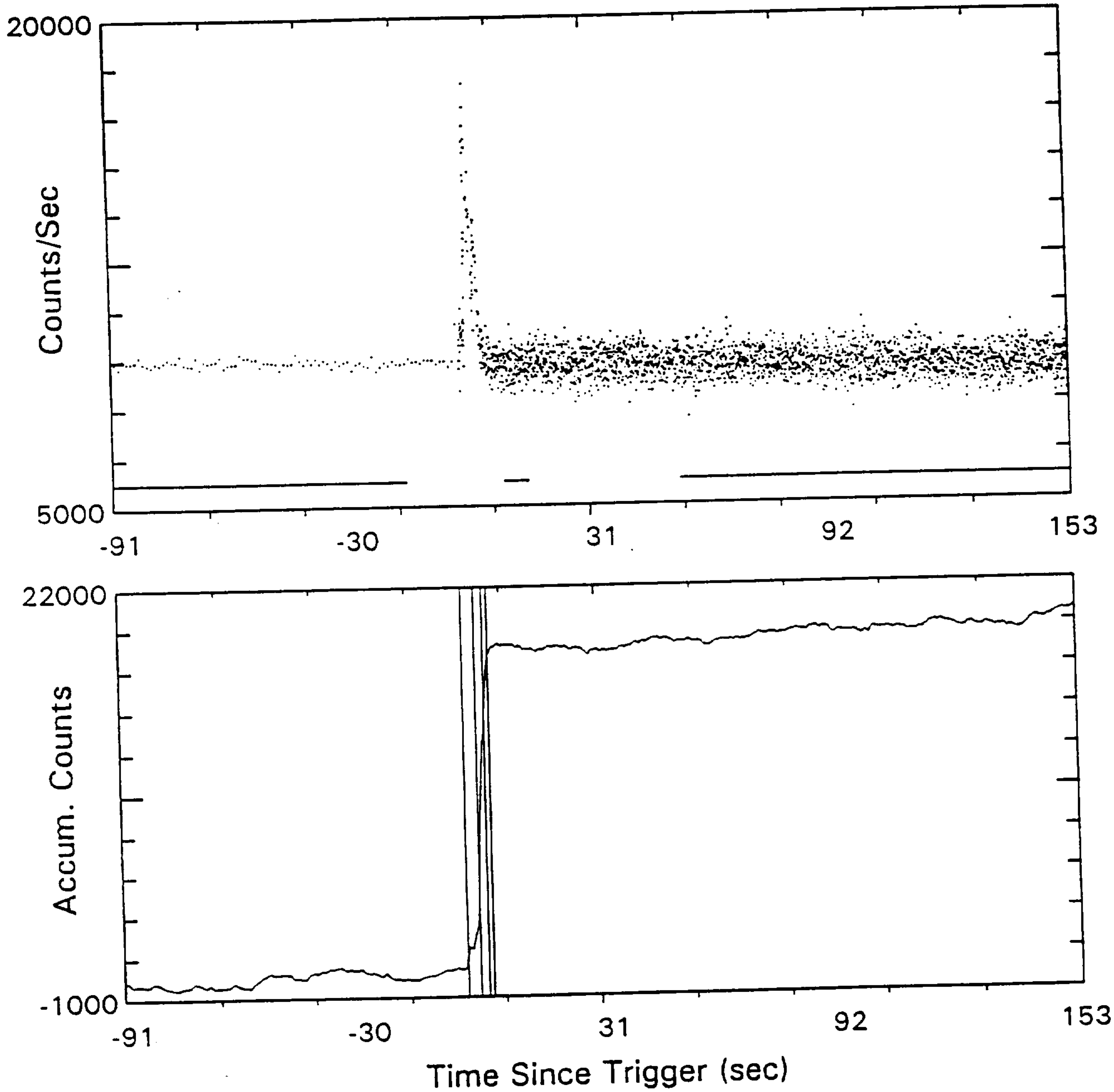

Bkgs=-90.82 to-16.06 8.8 to 15.392 53.86 to 152.61
Poly. Order= 2; Chisq= 212; (337, 363). Coefs below:
9332   -1.761   -4.570E-04   0.00E+00   0.00E+00
Start T_50 = 0s;   T_50 = 2.176s. +/-   0.202
Start T_90 =-3.264s;   T_90 = 6.688s. +/-   2.233

FI50=	3,145	3,626	3,372	226
FI90=	5,804	6,441	5,544	102

07-18-1996 15:07 lps_3177.   Rev. Asc1

Figure 1

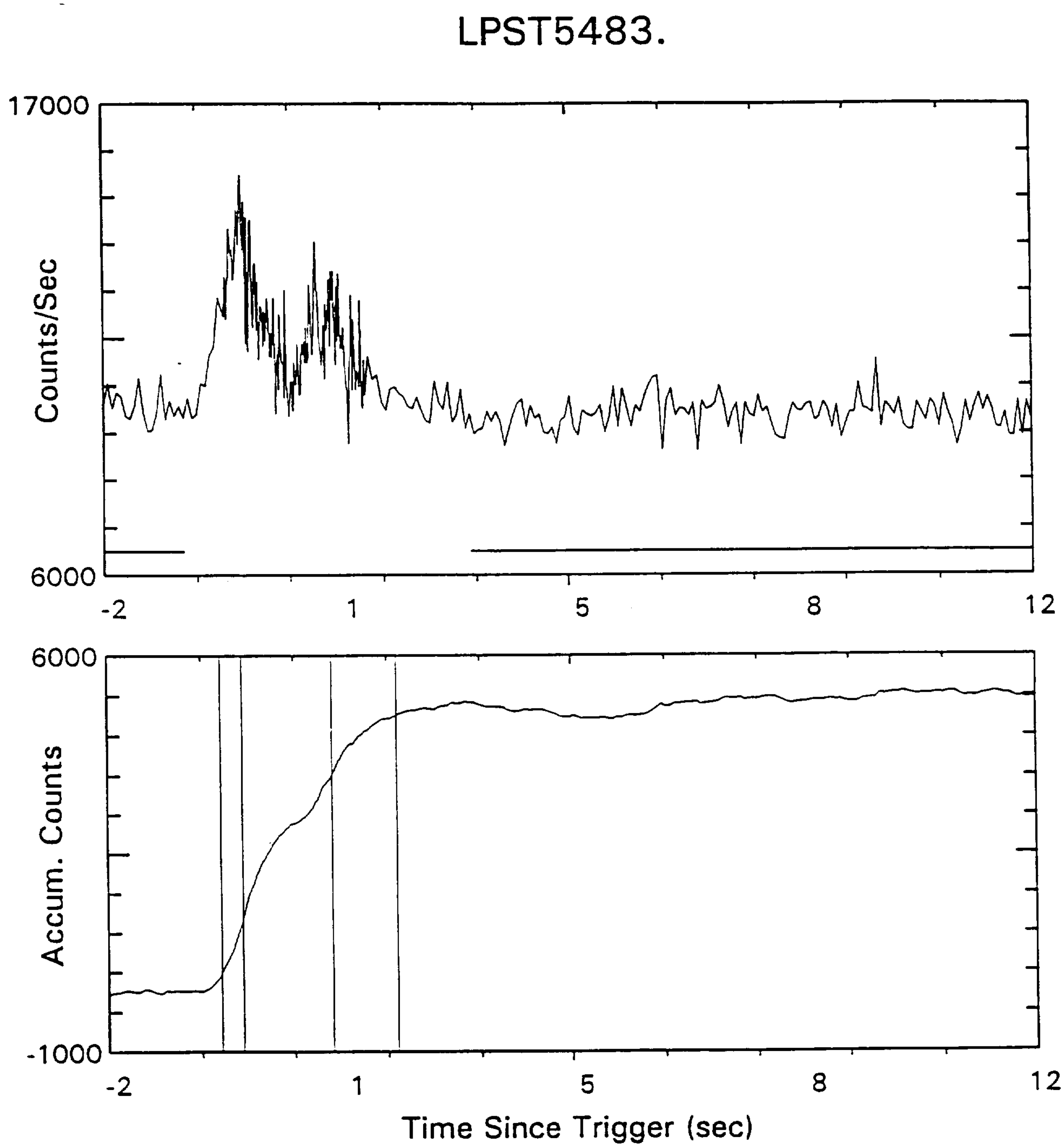

Bkgs=-1.888 to-.736 3.424 to 11.616 0 to 0
Poly. Order= 2; Chisq= 9; (24, 140). Coefs below:
9828 -31.166 2.061E+00 0.00E+00 0.00E+00
Start T_50 = .06s; T_50 = 1.312s. +/- 0.113
Start T_90 =-.256s; T_90 = 2.56s. +/- 0.580

FI50=	1,252	1,052	345	34
FI90=	2,129	1,976	774	-77

10-08-1996 14:17 lpst5483. Rev. bin-b

Figure 2

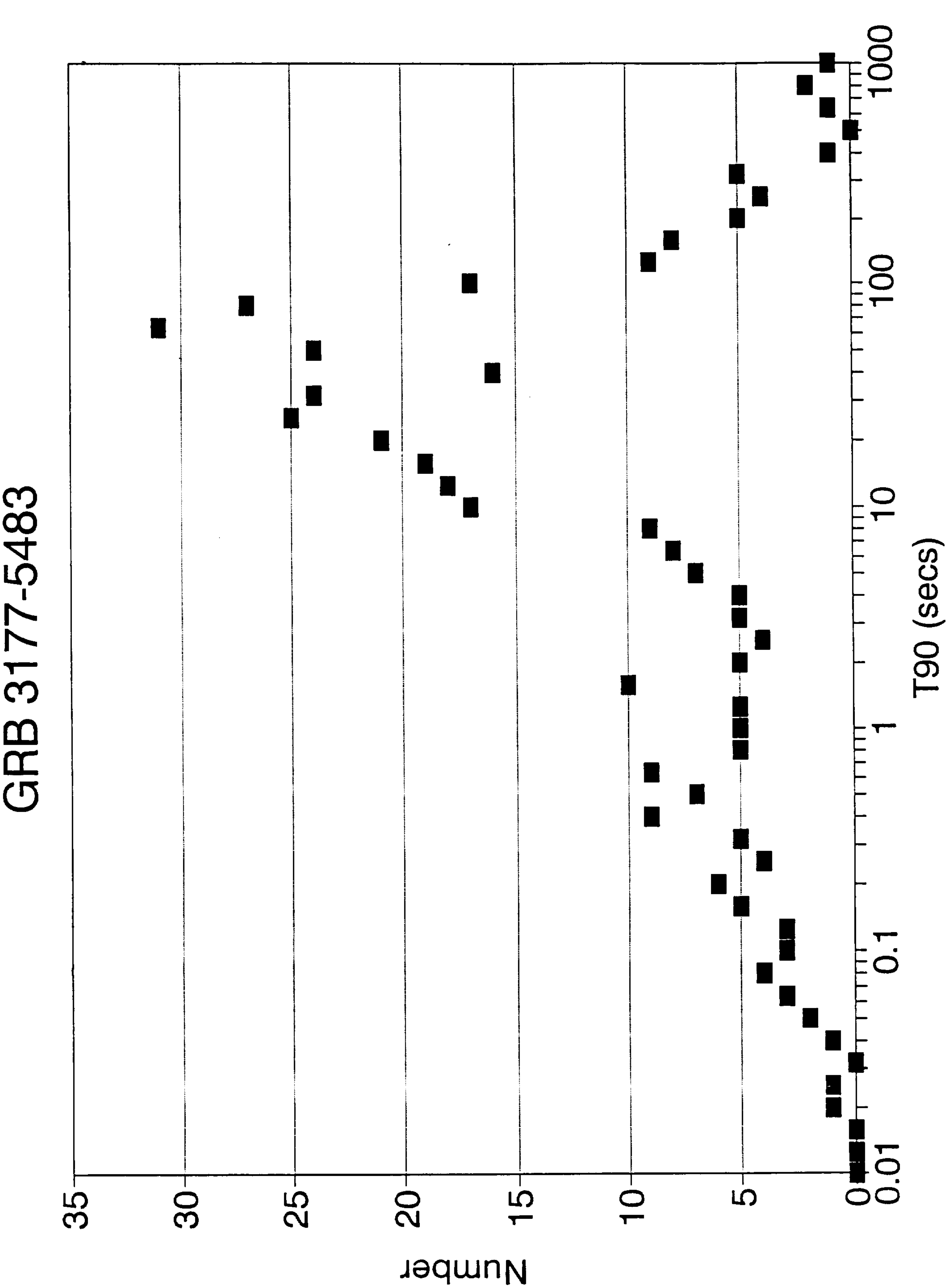
GRB 3177-5483
Number
T90 (secs)
0
5
10
15
20
25
30
35
0.01
0.1
1
10
100
1000

Figure 3

THE ASTROPHYSICAL JOURNAL, 471:L27–L30, 1996 November 1

THE HARDNESS-DURATION DIAGRAM OF GAMMA-RAY BURSTS

J. P. DEZALAY AND J. P. LESTRADE
Department of Physics and Astronomy, Mississippi State University, MS 39762
C. BARAT AND R. TALON
Centre d'Etude Spatiale des Rayonnements, CNRS/UPS, BP 4346, F-31029, Toulouse, France
AND
R. SUNYAEV, O. TEREKHOV, AND A. KUZNETSOV
Space Research Institute, Profsoyuznaya, 84/32, 117810 Moscow, Russia
Received 1996 May 31; accepted 1996 August 20

ABSTRACT

The hardness-duration diagram for gamma-ray bursts still contains undiscovered important information about the intrinsic properties of these phenomena. We analyze these diagrams for the PHEBUS and BATSE experiments. First, we show that the BATSE diagram is very similar to that for PHEBUS when we restrict the BATSE data set to events observable by PHEBUS. In this case, both diagrams present a high degree of clustering into two subclasses. This shows that the brightness of the events is a more important factor in determining the aspect of this diagram than the hardness ratio energy ranges. Second, for the subclass of long bright bursts, both experiments show evidence for a *positive* correlation between hardness and duration. This is a significant new result, as it represents an intrinsic property of long events. The commonly held perception of an anticorrelation (between hardness and duration) for all bursts must be replaced by a more complicated model that treats the two subclasses separately. No statistically significant correlation is found within the short-event population. The existence of such an intrinsic positive correlation for the long bursts would complicate the search for cosmological effects in the gamma-ray burst data.

Subject heading: gamma rays: bursts

1. INTRODUCTION

The most significant advances in our understanding of the nature of cosmic gamma-ray bursts (GRBs) have been made through statistical studies. Statistical studies of the position and of the intensity of bursts have restricted models of the spatial distribution of sources to either an extended galactic halo or a cosmological distribution. They are also the principal tool used to search for subclasses in the GRB population. To date, morphological studies of burst time profiles have not succeeded in exhibiting any classification schemes (Fishman & Meegan 1995; Lestrade 1994). The only strong evidence that subclasses of events exist comes from the durations of GRBs. The first piece of evidence is the bimodality of the duration distribution reported by several authors (Klebesadel 1992; Kouveliotou et al. 1993). The second is that the spectrum of short events is, on average, harder than that for longer events (Dezalay et al. 1992, 1995, 1996; Kouveliotou et al. 1993). At present no significant differences have been detected between the angular or intensity distributions of the two kinds of bursts. The only evidence we have that the population of GRBs may be divided into at least two subclasses lies in the hardness-duration diagram (HDD). This diagram could, therefore, be considered as a potential Hertzsprung-Russell diagram for GRBs. In the following, we compare the HDD from BATSE and PHEBUS, which are the only experiments presenting a significant difference between the average hardness of short and long bursts. We perform this analysis using the Third BATSE Catalog (Meegan et al. 1996) and the PHEBUS data set. We also study the hardness and duration distributions of short and long events separately in order to search for specific trends.

2. THE HARDNESS-DURATION DIAGRAMS

The qualitative comparison of the PHEBUS and BATSE HDDs gives the impression that the short-burst and long-burst populations are more separated in PHEBUS than they are in BATSE data. Although not statistically significant, this fact has to be investigated further, since one would have expected a larger separation in BATSE due to the stronger bimodality of the duration distribution. It is important to determine whether the different aspects of the two diagrams are due to the energy bands used to calculate the hardness, to the intensity of events, or to a smaller event sample in PHEBUS.

We calculated the durations of PHEBUS (Barat et al. 1988) events using the T_{90} algorithm by Kouveliotou et al. (1993). The major advantage of this integral criterion is that it gives measures that do not depend on the background level. Other measures were tried, including a differential one based on the intensity of the time profile above the background level (Dezalay et al. 1995). We find that the choice of the duration criterion has no effect on the shape of the the HDD or on the conclusions drawn from it. The bimodality is only slightly present in the distribution of PHEBUS T_{90} durations. This fact shows that the separation observed for the two HDD populations in PHEBUS is not the consequence of a strong bimodality. The hardness of PHEBUS events is calculated using the mean hardness ratio (MHR). It is derived from the count spectrum integrated over the 3 σ duration defined in Dezalay et al. (1995). The energy ranges used are 120–320 keV and 320–7000 keV. The distribution of the mean hardness ratios is unimodal. The HDD constructed using MHR and T_{90} is reported in Dezalay et al. (1996) and displayed in Figure 1*a*.

To compare PHEBUS and BATSE, we use the data pub-

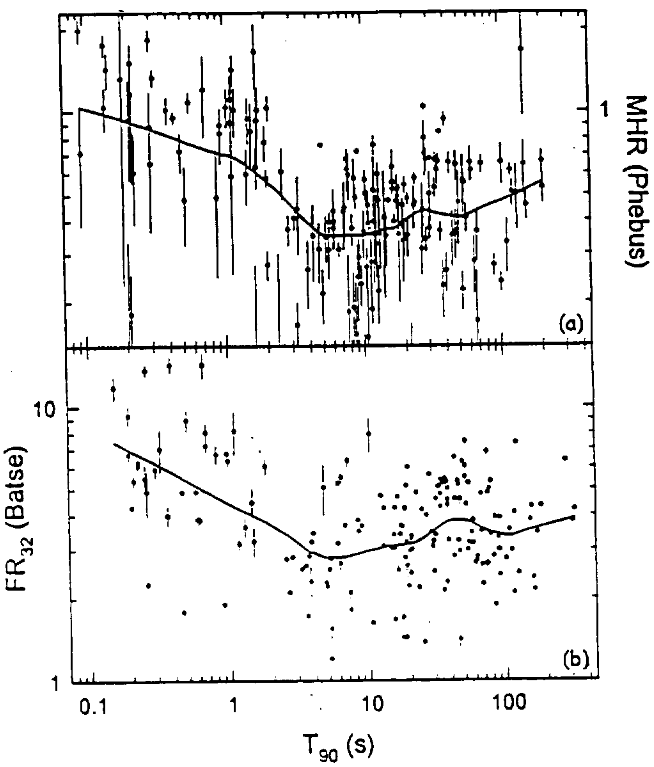

FIG. 1.—The solid line in each plot is the smoothed (40% Loess filter) line linking all points when ordered according to T_{90}. (*a*) HDD for PHEBUS. Eight PHEBUS bursts out of 174 are out of the vertical limits of the diagram. (*b*) HDD for type I (intense with $P_{256} > 2.8$ photons cm^{-2} s^{-1}) events. Six out of 178 type I events are not displayed.

lished in the Third BATSE Gamma-Ray Burst Catalog (3B Catalog) by Meegan et al. (1996). The hardness of BATSE events is measured using the ratio of fluences from different channels. Uncertainties associated with this quantity are larger than those of the hardness ratio (HR) of counts. To illustrate the difference between the two criteria, we compare the significance of the separation between the average hardness of short ($T_{90} < 2$ s) and long ($T_{90} > 2$ s) events of the 1B Catalog. Using HR_{32} (ratio of the total counts in the 100–300 keV energy range over those in the 50–100 keV range), Kouveliotou et al. (1993) reported that the difference in hardness is significant at a 7.3 σ confidence level. The same quantity calculated with the ratio of fluence 3 (100–300 keV) to fluence 2 (50–100 keV), FR_{32}, is only 2.2 σ. This result is explained mostly by the large uncertainties of the fluences of short bursts due to the deconvolution process on a small number of counts. The relative uncertainty of the average hardness of short events is 5% using HR_{32}, while it is 25% when calculated with FR_{32}.

In order to put the two experiments on an equal footing of sensitivity, we have to select only the most intense BATSE events. To this end, we used the peak flux on the 256 ms timescale (P_{256}) in the 50–300 keV energy range as our intensity criterion for BATSE. This timescale corresponds to the shortest trigger time interval in PHEBUS. Selecting the most intense bursts for BATSE according to P_{256} will affect events shorter than $\frac{1}{4}$ s the same way in BATSE as in PHEBUS. The 3B Catalog and the PHEBUS data set have 51 events in common. Among this sample, only 39 have an available measure of three quantities: T_{90}, fluence, and peak flux. The weakest of these 39 events has a peak flux equal to 2.8 photons cm^{-2} s^{-1}. In this paper we refer to the sample of BATSE bright bursts with a peak flux above this value as type I. It contains 178 events. Similarly, we construct two other BATSE samples according to their intensity: type II comprises 446 events with $0.6 < P_{256} < 2.8$ photons cm^{-2} s^{-1}, and type III has 178 events with $P_{256} < 0.6$ photons cm^{-2} s^{-1}.

As presented in Figure 1*b*, the HDD of BATSE type I bursts is qualitatively very similar to the PHEBUS HDD (Fig. 1*a*). To be able to compare the diagrams by eye more easily, we have smoothed the imaginary line linking all points (sorted according to their duration) using a weighted Loess filtering method. The trend of this smoothed line is similar for the BATSE type I and PHEBUS bursts and consists qualitatively of two connected power laws, the first with a negative power-law index up to $T_{90} \sim 5$ s, followed by the second with a positive slope. Although no quantitative information can be extracted from this smoothed line, it shows that the diagrams look similar even when different criteria are used to measure the hardness and different energy ranges to measure the duration. The positive trend observed within the long bursts suggests that a separate analysis for the two populations might prove fruitful.

3. CORRELATION BETWEEN HARDNESS AND DURATION

In this section we restrict our analysis to samples of long events ($T_{90} > 2$ s) detected by BATSE and PHEBUS. We calculate the significance of the positive trend observed in the HDD using two different statistical tests. We investigate the evolution of this correlation between spectral hardness and duration as a function of the intensity of bursts in the sample in BATSE. We also briefly discuss systematic effects that could affect these observations.

3.1. *Positive Correlation Hardness Ratio and T_{90} in Long and Bright Bursts*

Long and bright bursts ($T_{90} > 2$ s) from the BATSE type I and PHEBUS samples are displayed in the HDD in Figure 2. The significance of the trend observed in Figure 2 is estimated by the Spearman and the Kolmogorov-Smirnov (K-S) tests (Press et al. 1992). The Spearman rank-order test applied to PHEBUS long bursts (see Table 1) yields a correlation coefficient (Spearman rho) equal to 0.243. The probability ($P_{\rm Spear}$) that this correlation is due to a random fluctuation is 5.1×10^{-3} and corresponds to a 2.8 σ confidence level. The same test applied to the BATSE type I events yields a similar result with a correlation coefficient of 0.216, or 2.6 σ ($P_{\rm Spear} = 9.7 \times 10^{-3}$). Since the two results are independent, the probability of finding the same correlation in both PHEBUS and BATSE is equal to 5×10^{-5}.

Dividing the long bursts into two subsamples according to the median duration allows us to apply the K-S test. The hypothesis tested is that the hardness distributions of the two subsamples come from the same parent population. The K-S test confirms the result obtained with the Spearman test, i.e., that in bright and long bursts the spectral hardness is positively correlated with the duration. Results of both tests applied to the long bursts in each of the three BATSE samples and PHEBUS are summarized in Table 1.

If there is a correlation between T_{90} and brightness (Norris et al. 1996) associated with the well-known correlation between hardness and brightness (Atteia et al. 1994; Nemiroff et

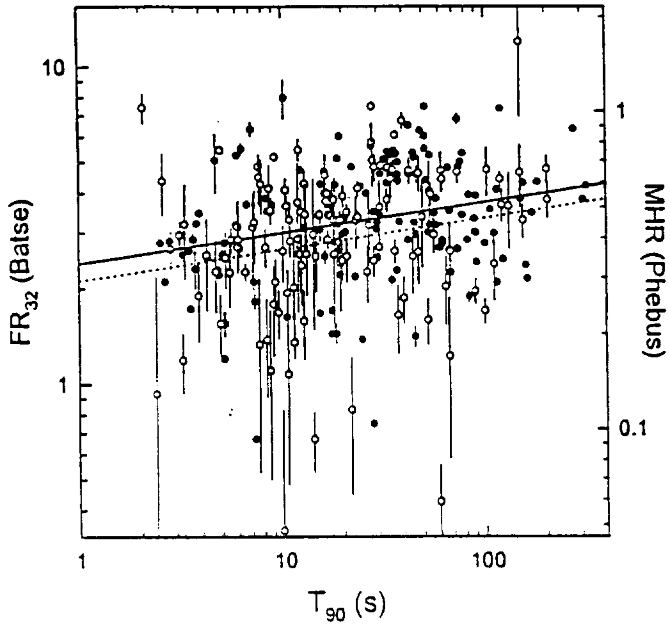

FIG. 2.—HDD for long ($T_{90} > 2$ s) PHEBUS bursts (*filled circles*) and BATSE type I bursts (*open circles*). The two lines represent the least-squares fits for BATSE (*solid line*) and PHEBUS (*dotted line*) events in the HDD.

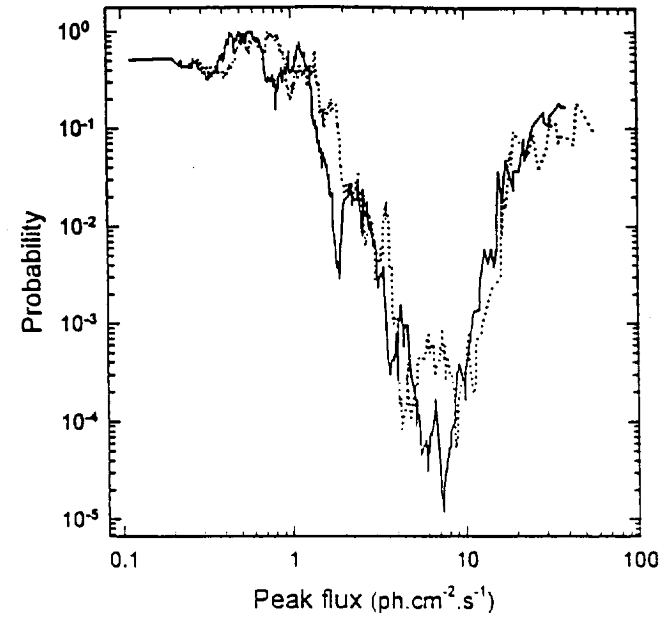

FIG. 3.—Probability $P_{\rm Spear}$ of obtaining, by chance, a positive correlation between FR_{32} and T_{90} for a sample of long BATSE bursts brighter than the threshold value of the peak flux (*abscissa*) on the 256 ms (*solid line*) and 1024 ms (*dotted line*) timescales.

al. 1994), it could result in a positive correlation between duration and hardness. However, a recent study by Koshut et al. (1996) of systematic effects on T_{90} shows that there is no systematic dependence of T_{90} on the burst signal-to-noise ratio for a sample of simulated and real time profiles. Moreover, if there is a correlation between T_{90} and intensity, it should also be observed in weaker burst samples when the brightness range is the same. This is not the case (see § 3.2). Therefore, since the correlation is still observable and even more significant using the brightest BATSE events, we think this result cannot be explained by selection or systematic effects in the data. We believe that we have identified for the first time an intrinsic property within the long-burst population. We are not aware of any theoretical model predicting a positive correlation between hardness and duration. On the other end, some models, e.g., Mészáros & Rees (1994), predict an anticorrelation between hardness and duration. However, there is no contradiction since they do not treat the two subclasses separately.

TABLE 1

STATISTICS OF THE FOUR SAMPLES

Statistic	PHEBUS	Type I	Type II	Type III
Number short/long[a]	43/131	34/144	139/307	35/143
Separation in hardness[b]	6.0	4.7	5.5	1.3
Spearman rho[c]	0.243	0.216	−0.109	0.063
$P_{\rm Spear}$	0.0051	0.0097	0.056	0.46
$P_{\rm KS}$	0.046	0.0060	0.088	0.30
With equal brightness range in BATSE				
Number short/long[a]	...	9/44	57/179	142/371
Spearman rho[c]	...	0.555	0.020	−0.027
$P_{\rm Spear}$	...	9.1×10^{-5}	0.79	0.60

[a] Using the $T_{90} = 2$ s boundary.
[b] Significance of the separation between the average hardness of short (<2 s) and long (>2 s) events.
[c] Spearman rank-order correlation coefficient.

3.2. *Evolution of the Correlation With Intensity*

We do not contend that the whole ensemble of bursts displays a positive correlation between burst hardness and duration. On the contrary, the correlation we find exists for only the nearest and brightest long GRBs. No significant correlation has been found in the weaker type II and III events (Table 1), or in the short-burst population. The three samples of bursts in BATSE were created to compare PHEBUS and BATSE. However, the range in the intensities of type I events is larger than that in type II and III samples. To check whether different ranges could affect the correlation, we performed the same analysis with three new samples having comparable ranges in brightness. Results summarized in Table 1 confirm that the correlation is still not observed in the two weaker event samples.

To take this analysis one step further, we have calculated the probability of finding a correlation in the long BATSE bursts by chance using different peak flux criteria. Figure 3 shows that as the peak flux threshold (on the 1024 and 256 ms timescales) is increased (meaning that we are selecting brighter and brighter bursts), the correlation between hardness and duration improves. The lowest probability observed is 10^{-5}. It is calculated using the ~50 brightest long BATSE events. When the value of ~7 photons cm^{-2} s^{-1} is reached for peak flux, only 46 long events remain. Past this value, the increase in probability is likely due to poor statistics. We have repeated this calculation for the peak flux integrated on 64 ms and found the same behavior. Figure 3 generalizes the results shown in Table 1, that the correlation increases with the average brightness of the long bursts. This evolution could be due to cosmological effects becoming more important for weaker events. At this time, we cannot exclude the possibility that the weakening of the correlation between spectral hardness and duration observed for long and bright bursts is caused by systematic effects.

4. CONCLUSIONS

We have shown that the HDD diagrams from PHEBUS and from a subsample of BATSE bright events are similar. This result tends to show that the difference in the energy ranges used to measure the hardness between the two experiments has very little influence on the aspect of the diagram. We have also found a positive correlation between the duration and the hardness in the samples of long and bright bursts detected by PHEBUS and BATSE. This correlation is not detectable in samples of long and weak events or in the short-event population. The different trends exhibited by the two subclasses in the diagram suggest that they should be studied separately. This result has an important implication for the research of cosmological effects in the data. For an extragalactic distribution of sources, we expect longer bursts to be weaker due to time dilation, and weaker events to be softer due to the redshift of the spectrum (Paczyński 1992). Therefore, since we find that within the long-burst population the longer events are harder on average, this result cannot be explained by cosmological effects. We believe that the correlation is an intrinsic property of the long-burst population. The presence in the data of such a correlation does not contradict or support the cosmological hypothesis, since it is observable only for bright events. Nevertheless, this correlation between hardness and duration may complicate the search for cosmological effects.

The positive correlation (hardness vs. duration) has been confirmed independently by Horack et al. (1996) using the 50 brightest bursts in the BATSE 3B Catalog.

We thank Tom Koshut (USRA) for fruitful discussions. We also acknowledge the help of James Berger (Purdue University) for his clustering analysis. J. P. L. was partially supported by NASA grant NCC8-82.

REFERENCES

Atteia, J.-L., et al. 1994, A&A, 288, 213
Barat, C., et al. 1988, in Nuclear Spectroscopy of Astrophysical Sources, Vol. 170, ed. G. H. Share & N. Gehrels (New York: AIP), 395
Dezalay, J.-P., et al. 1992, in AIP Conf. Proc. 265, Gamma-Ray Bursts, ed. W. S. Paciesas & G. J. Fishman (New York: AIP), 304
———. 1995, Ap&SS, 231, 115
———. 1996, AIP Conf. Proc., Third Huntsville GRB Workshop, in press
Fishman, G. J., & Meegan, C. A. 1995, ARA&A, 33, 415
Horack, J., et al. 1996, ApJ, submitted
Klebesadel, R. W. 1992, in Gamma-Ray Bursts, ed. C. Ho, R. I. Epstein, & E. E. Fenimore (Cambridge: Cambridge Univ. Press), 161
Koshut, T. M., et al. 1996, ApJ, 463, 570
Kouveliotou, C., et al. 1993, ApJ, 403, L101
Lestrade, J. P. 1994, ApJ, 429, L5
Meegan, C. A., et al. 1996, ApJS, in press
Mészáros, P., & Rees, M. J. 1994, in AIP Conf. Proc. 307, ed. G. J. Fishman, J. J. Brainerd, & K. Hurley (New York: AIP), 505
Nemiroff, R. J., et al. 1994, ApJ, 435, L133
Norris, J. P., et al. 1996, AIP Conf. Proc., Third Huntsville GRB Workshop (New York: AIP), in press
Paczyński, B. 1992, Nature, 355, 521
Press, W. H., et al. 1992, Numerical Recipes (2d ed.; Cambridge: Cambridge Univ. Press)

YUAN YAN

P.O.Box 3715
Miss. State, MS 39762, USA
(601) 325-8031; yy1@ra.msstate.edu

SPECIAL SKILLS

Physics Experiments, Scientific & Engineering Measurements, Electronics, Artificial Neural Networks, Fuzzy Logic Control.

EXPERIENCE

Research Assistant and Teaching Assistant:
For Lab-class Instruction & Lab Preparation.
at Mississippi State University (MSU) 1990 – Recent
at University of Texas at El Paso (UTEP) 1986 – 1989
Research Staff:
For Software and Hardware Development.
at Shanghai Institute of Process Automation Instrumentation (SIPAI). Before 1986

RESEARCH

Chaos and Multifractals in Gamma Ray Burst Time Profiles, Dissertation Research, MSU.
A Survey of Identifying Parameters For An Adaptive Comb Filter, Thesis For The Degree Of Master of Science, UTEP.
Nuclear Experiment And Instrumentation, UNISOR, Oak Ridge National Laboratory.

PUBLICATIONS

- Cosmic Gamma Ray Burst Time Profile: A Search For Cycles. Mississippi Academy of Science (MAS), 1995.
- A Multifractal Study of the Scaling Properties of Gamma Ray Burst Time Profiles. APS Proceedings for 3rd Huntsville Gamma Ray Burst Symposium, 1995 (in press).
- Scale Invariant Properties in Gamma Ray Burst Time Profiles Through Cascade Multiplier Analysis. SEA-APS, Tallahassee, Florida, 1995.
- An Alternate Way to Study the Multifractal Properties of Gamma Ray Burst Time Profiles. MAS, 1996.
- Evidence for Scale Invariance in Long Duration Gamma Ray Burst Time Profiles. MAS, 1997, submitted.

EDUCATION

Doctor of Philosophy, Engineering Physics,
Missiissippi State University, 1997, expected.
Master of Science , Physics,
University of Texas at El Paso, 1989.

COMPUTER LITERACY

UNIX, X WINDOW, INTERNET, CMS, MS-DOS;
C, FORTRAN, MATLAB, IDL, PASCAL, BASIC;
MATHCAD, QUATTRO PRO, MAPLE, NETLIB.

MEMBERSHIP

American Physical Society (APS).
Associate Membership, Sigma Xi, The Scientific Research Society.
UNISOR, Oak Ridge National Laboratory.

REFERENCES

Available upon request.